Available online at www.sciencedirect.com
SCIENCE DIRECT
Journal of Power Sources 158 (2006) 614–619
JOURNAL OF POWER SOURCES
www.elsevier.com/locate/jpowsour

Study of multiple interactions in mesoporous composite PEO electrolytes

M. Jaipal Reddy [a,*], Peter P. Chu [b], U.V. Subba Rao [a]

[a] *Department of Physics, Osmania University, Hyderabad 500007, India*
[b] *Department of Chemistry, National Central University, Chung-Li 32054, Taiwan, ROC*

Received 31 August 2005; received in revised form 30 September 2005; accepted 3 October 2005
Available online 22 November 2005

Abstract

This paper discusses the FT-infrared (IR) and NMR spectroscopy results of a mesoporous silica (SBA-15) composite poly(ethylene oxide) (PEO) solid lithium polymer electrolyte. The changes in COC, CH, and ClO_4 stretching IR vibrational modes indicated a combination of multiple interactions through Lewis acid–base reactions which interrupt the PEO crystalline structure. Higher salt disassociation by SBA-15 is also apparent from ClO_4 vibrational band mode.

NMR studies indicated three types of Li ion environments; the first one is Li ions within the conventional amorphous PEO, the second is Li ions on the surface of mesoporous SBA-15 and the third is Li ions trapped along with PEO in the nano-tubular channels of SBA-15. Annealing leads to interaction of more PEO and lithium ions with the SBA-15 and free ions for conduction, as reflected in the ^{7}Li variable temperature (VT)-NMR measurements and variable temperature ion conductivity.

Keywords: Composite polymer electrolyte; Poly(ethylene oxide); $LiClO_4$; SBA-15; Infrared; NMR

1. Introduction

Intensive interest in inorganic–organic polymeric composite electrolytes arises owing to their merits in solid-state electrochemical devices such as higher ionic conductivity, mechanical strength, and stronger contact with electrodes in devices. The basic idea of dispersing an inorganic oxide filler in a polymer electrolyte matrix is to create a high degree of disorder [1–3]. The role of the filler in terms of the Lewis acid–base model interaction is to provide filler surface groups as physical cross-linking centers for the PEO segments, and thus reduce the polymer reorganization tendency which establishes additional conducting pathways on the filler surface [4–6].

MCM-41 is a mesoporous material, which has a large surface area, and is composed of stacking SiO_2 channels arranged in the hexagonal array with pore sizes ranging from 2 to 10 nm [7]. SBA-15 is also a mesoporous silica with uniform, long, connecting tubular channels of variable pore sizes from 5 to 30 nm and large surface area [8]. Mesoporous MCM-41 and SBA-15 have been used in the formation of composite polymer electrolytes with a PEO polymer and a lithium salt [9,10]. These results confirmed PEO and mesoporous silica exhibit good inter-phase interactions (i.e., miscibility) in the presence of the lithium salt which enhanced the compatibility of the organic and inorganic moieties. The results also show that lithium has a stronger interaction with mesoporous SiO_2. The present paper is an extension of our earlier work to evaluate the interactions in PEO polymer-inorganic mesoporous silica (SBA-15) composites of the lithium polymer electrolyte by using infrared (IR), ^{7}Li variable temperature (VT)-NMR spectroscopy measurements.

2. Experimental

A mesoporous composite polymer electrolyte system has been prepared by using poly(ethylene oxide) (PEO) [MW: 2×10^5, Aldrich] with $LiClO_4$ salt in a 90:10 ratio blending with the different weight percentages of SBA-15 [10]. Initially, the PEO was dissolved in tetrahydrofuran (THF) followed by the addition of an appropriate amount of $LiClO_4$ salt and SBA-15 in 2 h intervals and stirring for 24 h at 60 °C. The homogeneous

* Corresponding author.
E-mail address: mjaipalreddy@yahoo.com (M.J. Reddy).

0378-7753/$ – see front matter © 2005 Elsevier B.V. All rights reserved.
doi:10.1016/j.jpowsour.2005.10.008

mixtures were poured into Teflon dishes and evaporated slowly at 40 °C in a vacuum. Further drying was conducted in a dry-box under nitrogen atmosphere to remove the solvent completely. All the samples were stored in a dry-box with a nitrogen atmosphere for protection from moisture.

The coordination of the $LiClO_4$ salt and nano-tubular pore channeled SBA-15 in PEO was investigated with the help of infrared spectroscopy. The IR spectra of all these films were recorded by using the BIO-RAD FT-IR spectrometer [FTS-155].

Solid-state ^7Li magic angle spinning (MAS) NMR spectra were recorded at variable temperatures on a Bruker DSX-300 spectrometer, operating at a resonance frequency of 116.6 MHz. A spinning speed of 2 kHz was employed, which is sufficient to remove the small shift anisotropy side bands to avoid major complications.

3. Results

Fig. 1 shows the FT-IR spectra of different compositions of mesoporous SBA-15 in PEO:$LiClO_4$. Of particular interest are the changes in intensity, shape and position of CH, COC and ClO_4^- IR bands, which reflect the multiple interactions like the ether oxygen of PEO with lithium ions, as well as SBA with lithium ions and PEO. The prominent vibrational spectral bands in PEO are CH (~2900 cm^{-1}) and COC, asymmetric and symmetric stretching modes, and C–O–C deformation modes (range between 900 and 1200 cm^{-1}) [11,12]. The aliphatic CH stretching vibrational band (ca. 2900 cm^{-1}) shows a decrease in intensity and width by the addition of lithium salt, and is further severely affected upon incorporation of mesoporous SBA-15. If the cations were coordinated with the ether oxygen of PEO, changes in the ether oxygen vibrational modes, such as C–O–C asymmetric and symmetric stretching modes, and deformation modes in the range of 900–1200 cm^{-1} [11–14] are expected. It is apparent that broad COC symmetric and asymmetric stretching mode width around 1150 cm^{-1} is severely decreased in the composite of lithium salt and SBA-15 in PEO. Not only is there a decrease in the COC mode width but also its maximum shifts to a lower wave-number when compared to pure PEO and pure PEO:$LiClO_4$ complex films. The downshift in the COC stretch suggests the formation of multiple interactions through cross-links within the composite electrolyte.

Fig. 2 shows the IR spectra of various compositions of PEO:$LiClO_4$/SBA-15 in the range of 600–650 cm^{-1}. This band has been assigned to the stretching of ClO_4^- ions, and is conveniently used to identify the degree of ion pairing. The shoulder peak at ~635 cm^{-1} is apparent in lithium salt containing PEO complex films. The asymmetric IR line shapes can be de-convoluted into two components. Agreements in the fit are demonstrated by the sample containing 10 wt.% of $LiClO_4$ as shown in Fig. 2(a). Based upon prior assignments, these peaks corresponds to two major ClO_4^- species with different conformations; one being free ClO_4^- ions with a maxima at ~623 cm^{-1} (denoted as 'i') and the other, ClO_4^- ion associated with the cation Li^+ at ~635 cm^{-1} (denoted as 'ii'). Wieczorek et al. [15] and Salmon et al. [16] have attributed similarly, the 623 cm^{-1} band to free anions ClO_4^- and 635 cm^{-1} envelope to ion pair formation or contact of anion ClO_4^- with lithium. Interestingly, the ion pair formation peak 'ii' has been suppressed

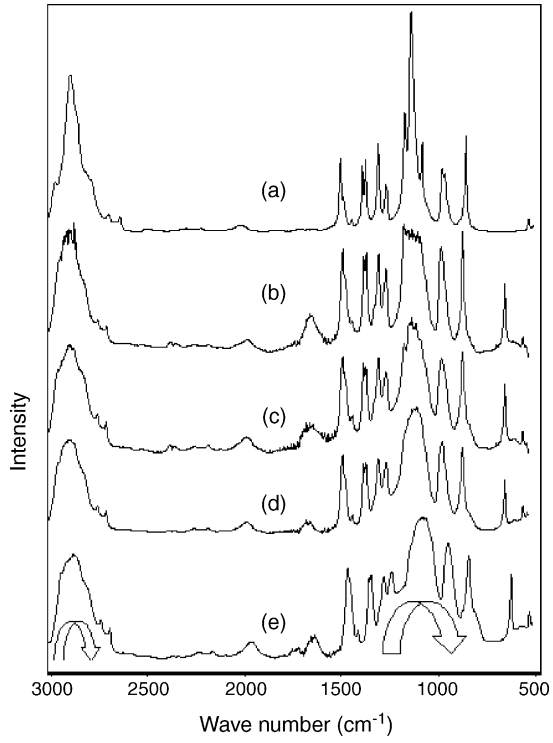

Fig. 1. FT-IR spectra of (a) PEO; (b) PEO:$LiClO_4$ (90:10); (c) 5; (d) 10; and (e) 15 wt.% of SBA-15 in PEO:$LiClO_4$.

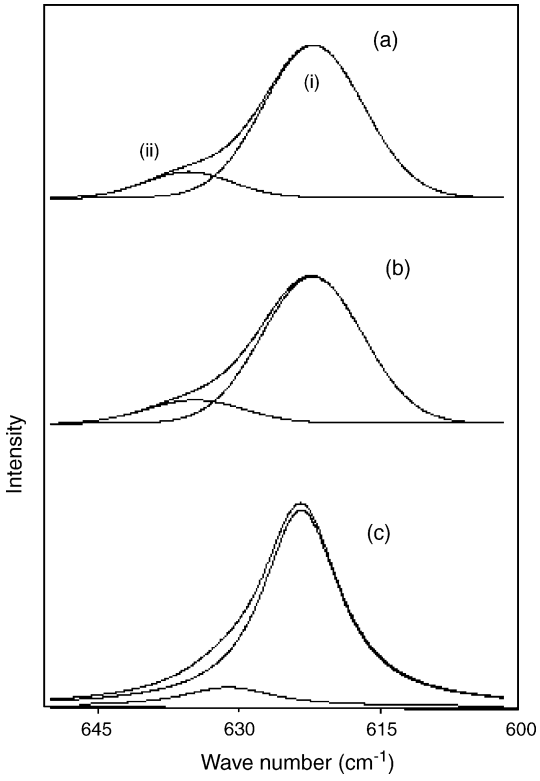

Fig. 2. FT-IR spectra of (a) PEO:$LiClO_4$ (90:10); (b) 5; and (c) 10 wt.% of SBA-15 in PEO:$LiClO_4$.

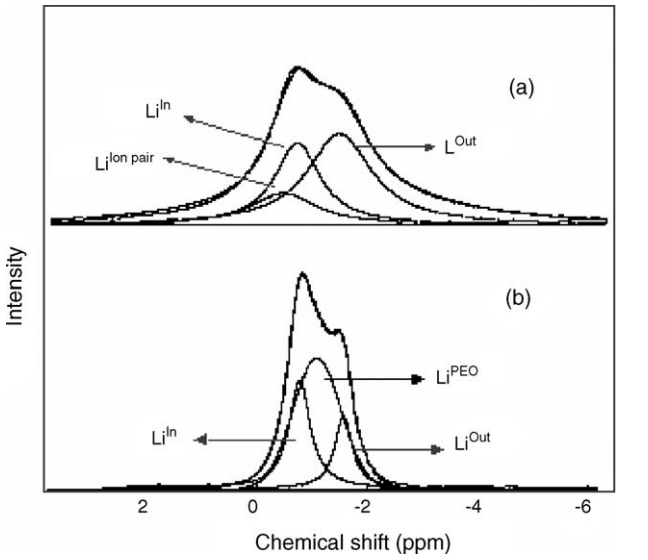

Fig. 3. Least square peak fits of ^{7}Li NMR spectra of (a) SBA-15:$LiClO_4$ (1:1 wt.%); and (b) 8 wt.% of SBA-15 in PEO:$LiClO_4$.

upon addition of SBA-15 to PEO:$LiClO_4$, which suggests that SBA-15 inhibits ion pair formation.

Solid-state ^{7}Li NMR study is a powerful tool to examine the coordination structure of lithium in the compound. In Fig. 3, the downfield peak '0' (near ~0.0 ppm) is conveniently assigned to the Li species of an un-dissociated salt, and the two upfield peaks, the middle 'Li^{In}' and higher 'Li^{Out}', are therefore assigned to lithium ions coordinated on the interior channel surface and on the outer surface of SBA-15, respectively [10]. The peak fits are noted as site 'Li^{Out}', 'Li^{In}', and 'Li^{PEO}', where site 'Li^{Out}' represents the lithium species on outer surface (0.5–0.7 ppm); site 'Li^{In}' as lithium species interior pore channels (1.1–1.5 ppm) of SBA-15 as previously assigned and site 'Li^{PEO}' represents lithium species with amorphous PEO (0.8–1.0 ppm). The lithium species with SBA-15 content shows an interesting trend: components of 'Li^{Out}' and 'Li^{In}' increase dramatically and 'Li^{PEO}' decreases with increase of SBA-15 in PEO:$LiClO_4$. This analysis indicated that lithium favors the association with SBA-15 over PEO, since stronger Li:SBA-15 peaks developed with increasing of SBA-15. This confirms that mesoporous structured SiO_2 raises the possibility of the development of a SBA-15:Li rich phase at higher SBA-15 compositions. The SEM, DSC and ionic conductivity results [10], indicated that the formation of the organic–inorganic complex is better in the inter-mediate compositions but phase aggregations occur above the composition of 10 wt.% SBA where the aggregation forms larger mesoporous lithium-rich domains.

Useful information on the ^{7}Li dynamics and kinetics is derived from the variable temperature-NMR (VT-NMR) measurement line widths for the lithium (−1/2 to 1/2) transition over the temperature range 298–373 K. The ^{7}Li line width spectra at different temperatures for the SBA (15 wt.%) in PEO:$LiClO_4$ is depicted in Fig. 4. With increase of temperature, the spectra begin to narrow in line width. These spectra are de-convoluted by least square fit into three components as described above to interpret individual components of three environments with

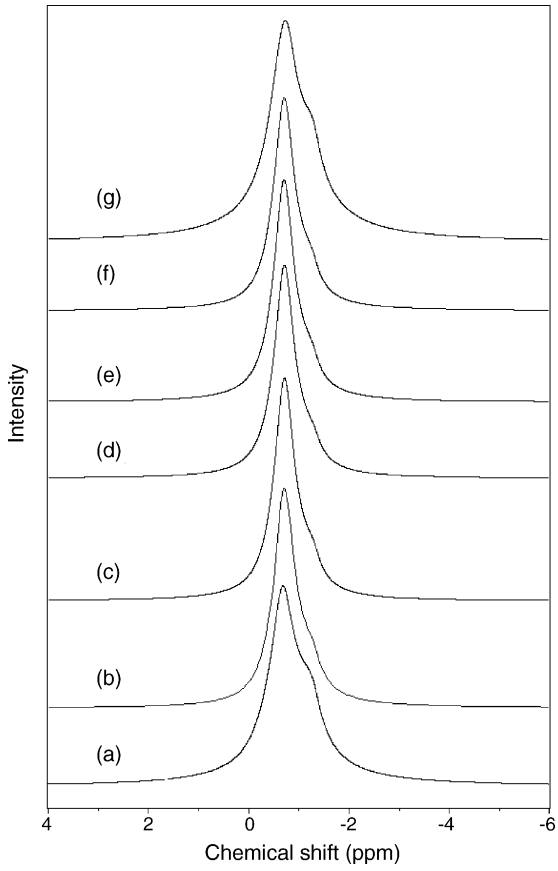

Fig. 4. Variable temperature ^{7}Li NMR spectra of 15 wt.% of SBA-15 in PEO:$LiClO_4$ (a) 298 K; (b) 323 K; (c) 343 K; (d) 373 K; while heating and (e) 343 K; (f) 323 K; (g) 298 K while cooling.

temperature while heating and cooling. The obtained line widths for these three components are shown in Fig. 5. The purpose of this finding is to explore how the lithium flux is exchanging between three components with temperature while heating and cooling above and below the melting temperature of the PEO. From the Fig. 5, it is clear that line width of the lithium flux in PEO is becoming narrow and other two components are also decreased in line width up to the melting temperature (T_m) and

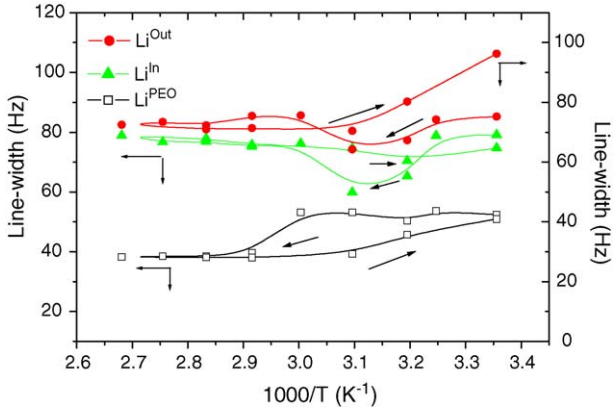

Fig. 5. Variable temperature line widths of lithium ion species of 15 wt.% of SBA-15 in PEO:$LiClO_4$.

regains again in their line widths. The cooling curve is not following its original path as heating, which corroborates well with the conductivity measurements while heating and cooling [10]. This suggests that the lithium ions are exchanging tremendously between amorphous PEO and mesoporous oxide. Motional narrowing begins when the rate of the fluctuations of the local dipolar fields or the electric field gradient (EFG) is comparable to their rigid lattice line width (Δ_{RL}) when $1/\tau_c \sim \Delta_{RL}$. Where τ_c is the motional correlation time. That is, the narrow component due to the dipolar interaction undergoes motional narrowing at the melting temperature of the polymer. The NMR line shape is narrowed with increasing temperature and could fit a Lorentzian line shape where the fwhm (Δ_{LW}) is a well defined parameter in terms of the spin–spin relaxation time (T_2),

$$\Delta_{LW} = \frac{1}{(\pi T_2)} \quad (1)$$

The fitting values of T_2 for three lithium environments with increasing temperature are shown in Fig. 6(a) for the 15 wt.% of SBA in PEO:$LiClO_4$. The results are found to be sensitive to the temperature. The T_2 maximum occurs at different temperatures for three components, demonstrating the difference in

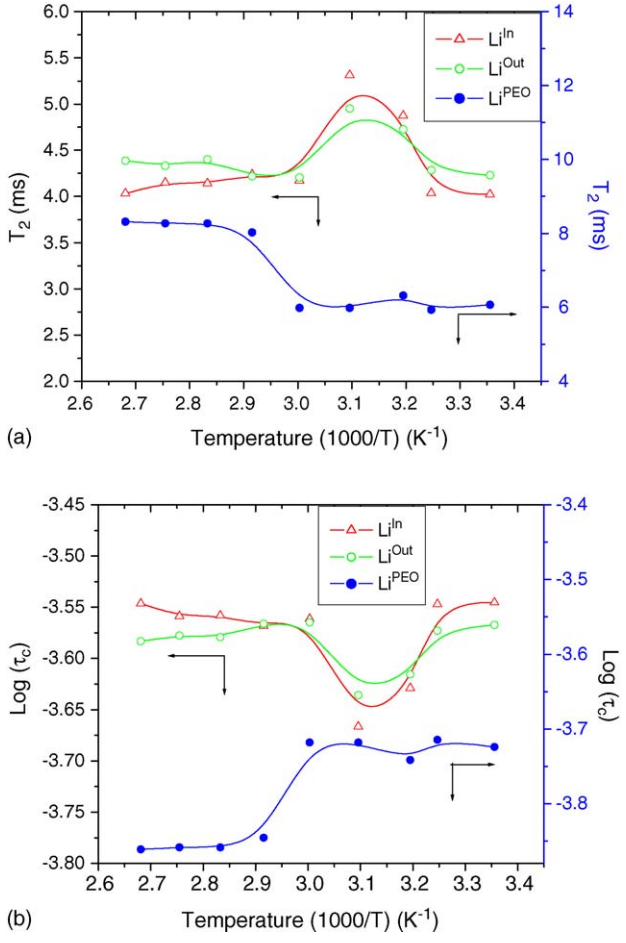

Fig. 6. (a) Variable temperature spin–spin relaxation time (T_2) of lithium ion species of 15 wt.% of SBA-15 in PEO:$LiClO_4$. (b) Variable temperature motional correlation time (τ_c) of lithium ion species of 15 wt.% of SBA-15 in PEO:$LiClO_4$.

Table 1
Activation energies of SBA-15 composite PEO:$LiClO_4$ electrolyte system

SBA-15 content (wt.%)	Lithium species	Activation energies (ΔE_a) (kJ mol^{-1})	
		Region I	Region II
8	Li^{PEO}	7.68	1.46
	Li^{In}	6.72	0.49
	Li^{Out}	3.61	0.39
15	Li^{PEO}	0.41	0.50
	Li^{In}	3.95	0.39
	Li^{Out}	2.21	0.57

Li correlation time. The changes in relaxation time indicate that all samples are governed by a diffusion mechanism [17]. The pseudo activation energy (ΔE_a) of lithium components in each lithium coordination environment is different. Activation energy (ΔE_a) for narrowing of line-width process can be evaluated by the following relationship [18]

$$\tau_c = \left(\frac{\alpha}{\Delta_{LW}}\right) \tan\left[\left(\frac{\pi}{2}\right)\left(\frac{\Delta_{LW}}{\Delta_{RL}}\right)^2\right] \quad (2)$$

where α is a parameter with order of unity. The τ_c values obtained by fitting in Eq. (2) is plotted with inverse temperature which shown as Fig. 6(b). Assuming τ_c to be thermally activated,

$$\tau_c = \tau_0 \exp\left(\frac{\Delta E_a}{kT}\right) \quad (3)$$

where τ_0 is the dwell time. The activation energies obtained by fitting in Eqs. (2) and (3) are summarized in Table 1. The activation energies measured for both regions are different. It is noted that the activation energies in region II is smaller than the region I. The activation energies are also smaller in higher content SBA-15 polymer electrolytes compared to lower content SBA-15 in PEO:$LiClO_4$.

4. Discussion

Mesoporous SiO_2 (SBA-15):PEO complex in presence of lithium salt shows good compatibility between the polymer and the inorganic moieties due to interactions between the three components in the composite. These interactions are responsible for reduction of crystallinity, a stable structure and favorable ion conductivity. FT-IR and NMR indicated that lithium exhibits a stronger association with SBA than the PEO, which is evident from the COC stretching mode maxima shifted to a lower wave-number in the SBA-15 composite electrolyte than in pure $LiClO_4$ in PEO. It is apparent that the effect of SBA-15 is to increase the fraction of available coordination sites in the composite electrolyte. The enhancement in lithium ions is observed from ClO_4^- vibrational mode corresponding to a lowering of the fraction of contact-ion pairs, which is lithium ions in the vicinity of the coordination with SBA-15. This result is consistent with the previous results reported [15,19], where the fraction of ion pairs is lower in the α-Al_2O_3 composite PEG–$LiClO_4$ and PEO–$LiClO_4$ electrolyte system compared to their pure electrolytes.

An ambient temperature ^{7}Li NMR result of mesoporous SBA-15 composite PEO electrolyte shows stronger association of lithium ion with SBA-15 than polymer PEO [10]. Interactions in PEO composite electrolytes can be accounted for by means of electrostatics, where Li^+ cations will experience a relatively stable potential landscape on the filler surface, which will be same order as that at the polymer [20]. Then the lithium ion will be free to move by segmental motion and activated hopping, with a potential barrier, which has been lowered by the filler. It is interesting that SBA-15 has larger channel dimensions which favor the occlusion of the PEO polymer along with the lithium ions into interior pore channels of SBA-15. The oxygen atoms in polymer PEO and mesoporous SBA-15 serve as the Lewis base centers, and the Li^+ cation as a strong Lewis acid. Possibly, silica in SBA-15 is acting as a Lewis acid center to physical cross-link by weak electrostatic interaction with the base center of ether oxygen of polymer PEO. This electrostatic interaction drives the occlusion of PEO and Li^+ ions into the hallow channels. The Lewis acid of the added oxide filler would compete with the Lewis acid character of the lithium cations to form new complexes with the PEO chains [21,22]. Thus, the filler oxide would act as cross-linking centers for the PEO chains. Such character lowers the polymer reorganization tendency and promotes an overall mechanically stable structure. The structure modification provides a new lithium ion environment on the filler surface as a salient feature attributed to the more free lithium ions to be mobile. Wong et al. [23] reports that the interactions of polymer and cation with the surface oxygen atoms occurred in the silicate layer. The occlusion of polymer PEO in the pore channels of SBA-15 is plausible where the silica and ether oxygen of polymer can interact with weak electrostatic interaction [24]. Melosh et al. [25], have reported that the block copolymer acts as a structure-directing agent where the silica cation preferentially associates with PEO blocks.

The activation energies of lithium species (E_a) are smaller in the higher content SBA composite compared to the lower content SBA-15 in PEO:$LiClO_4$. This suggests that the lithium ions are more with SBA-15 than amorphous PEO in high content SBA in PEO:$LiClO_4$, where larger lithium ion SBA-15 aggregation is apparent [10]. The activation energies, indicate two types of lithium ion mechanism in SBA composite electrolytes, which is different from the conventional pure PEO electrolytes. The basic motion of lithium ions in amorphous PEO is due to segmental motion and other established by lithium ion replacing nearby vacancies ('hole') on the SBA-15 surface (both interior and exterior).

The lithium flux is exchanging in between SBA-15 and amorphous PEO while heating and cooling. Line widths in the cooling curves for the lithium fluxes of Li^{PEO}, Li^{In}, and Li^{Out} are not following the same paths as heating (see Fig. 5). This suggests that the specific interaction between PEO and SBA-15 is severely affected after melting the polymer. Upon heating and cooling, the PEO is unable to recover its original structure. According to Croce et al. [26], once composite electrolytes are annealed at a temperature above the PEO melt, the larger surface area of the added filler prevents local PEO chain reorganization, so that a high degree of disorder is attained at ambient temperature. Annealing creates a large number of thermally induced defects at the polymer–filler interface [27]. These defects accommodate and facilitate lithium ions in the conduction process. Significantly, in this composite electrolyte, the mesoporous SBA served as both the filler and to tie molecules to improve the miscibility with PEO and $LiClO_4$ through physical cross-links and occlusion of polymer and lithium ions into pore channels of SBA-15.

5. Conclusions

The changes in COC, CH, and ClO_4 stretching IR vibrational modes and NMR studies of SBA-15 mesoporous composite PEO electrolyte system indicated three types of Li ion environments: (i) Li ions within the conventional amorphous PEO; (ii) Li ions on the surface of mesoporous SBA-15; and (iii) Li ions occlused along with PEO in the nano channels of SBA-15. The enhancement in lithium ions corresponds to a lowering of the fraction of contact-ion pairs with the inclusion of SBA-15 in PEO:$LiClO_4$. The ion conductivity of the mesoporous composite PEO:$LiClO_4$ increases with SBA-15 content and an optimum value is found at 10 wt.% of SBA-15 with one order improvement compared to the PEO:$LiClO_4$ electrolyte.

Acknowledgement

Author M. Jaipal Reddy thanks Council of Scientific and Industrial Research (CSIR), New Delhi, India for providing financial support in the form of SRA, under Pool Scientist's Scheme. The authors MJR and PPC wish to thank the National Science Council, Taiwan for the award of research project to carryout the experimental work.

References

[1] F. Croce, G.B. Appetechi, L. Persi, B. Scrosati, Nature 373 (1995) 557.
[2] F. Croce, F. Serraino Fiory, L. Persi, B. Scrosati, Electrochem. Solid-State Lett. 4 (2001) A121.
[3] B. Kumar, L.G. Scanlon, J. Electroceram. 5 (2) (2000) 127.
[4] W. Wieczorek, J.R. Stevens, Z. Florjanczyk, Solid State Ionics 85 (1996) 76.
[5] F. Croce, L. Persi, B. Scrosati, F. Serraino-Fiory, E. Plichta, M.A. Hendrickson, Electrochim. Acta 46 (2001) 2457.
[6] S.H. Chung, Y. Wang, L. Persi, F. Croce, S.G. Greenbaum, B. Scrosati, E. Plichta, J. Power Sources 97–98 (2001) 644.
[7] A. Corma, Chem. Rev. 97 (1997) 2373.
[8] D. Zha, Q. Huo, J. Feng, B.F. Chmelka, G.D. Stucky, J. Am. Chem. Soc. 120 (1998) 6024.
[9] P.P. Chu, M. Jaipal Reddy, H.M. Kao, Solid State Ionics 156 (2003) 141.
[10] M. Jaipal Reddy, P.P. Chu, J. Power Sources 135 (2004) 1.
[11] M. Jaipal Reddy, P.P. Chu, J. Power Sources 109 (2002) 340.
[12] P.P. Chu, M. Jaipal Reddy, Tsai Joyce, Polym. Sci. Part B: Polym. Phys. 42 (2004) 3866.
[13] B.L. Papke, M.A. Ratner, D.F. Shriver, J. Phys. Chem. Solids 42 (1981) 493.
[14] S.A. Hashmi, A. Kumar, K.K. Maurya, S. Chandra, J. Phys. D 23 (1990) 784.
[15] W. Wieczorek, P. Lipka, G. Zukowska, H. Wycislik, J. Phys. Chem. B 102 (1998) 6968.

[16] M. Salomon, M. Xu, E.M. Eyring, S. Petrucci, J. Phys. Chem. 98 (1994) 8234.
[17] P.P. Chu, J. Hsiu-Ping, L. Fang-Rey, C.L. Lang, Macromolecules 32 (2000) 4738.
[18] A. Abargram, The Principle of Nuclear Magnetism, Clarendon, Oxford, 1983.
[19] W. Wieczorek, D. Raducha, A. Zalewska, J.R. Stevens, J. Phys. Chem. B 102 (1998) 8725.
[20] A.S. Best, J. Adebahr, P. Jacobson, D.R. Mac Farlane, M. Forsyth, Macromolecules 34 (2000) 4549.
[21] J. Przyluski, M. Siekierski, W. Wiezorek, Electrochim. Acta 40 (1995) 2101.
[22] W. Wiezorek, Z. Florjancyk, J.R. Stevens, Electrochim. Acta 40 (1995) 2251.
[23] S. Wong, R.A. Vaia, E.P. Giannelis, D.B. Zax, Solid State Ionics 86–88 (1996) 547.
[24] M. Imperor-Clerc, P. Davidson, A. Davidson, J. Am. Chem. Soc. 122 (2000) 11925.
[25] N.A. Melosh, P. Lipic, F.S. Bates, F. Wudl, G.D. Stucky, G.H. Fredrickson, B.F. Chemlka, Macromolecules 32 (1999) 4332.
[26] F. Croce, R. Curini, A. Marinelli, L. Persi, F. Ronic, B. Scrosati, R. Caminiti, J. Phys. Chem. B 103 (1999) 10632.
[27] B. Kumar, L.G. Scanlon, J. Electroceramic. 5 (2) (2000) 127.